Behavioural Brain Research 423 (2022) 113745

Contents lists available at ScienceDirect

Behavioural Brain Research

journal homepage: www.elsevier.com/locate/bbr

Activation of noradrenergic locus coeruleus and social behavior network nuclei varies with duration of male midshipman advertisement calls

Zachary N. Ghahramani [a,c,d,*], Jonathan T. Perelmuter [b,c,e], Joshua Varughese [c], Phoo Kyaw [c], William C. Palmer [g], Joseph A. Sisneros [g,h,i], Paul M. Forlano [c,d,e,f,**]

[a] Department of Biological Sciences, University of Mary Washington, Fredericksburg, VA, USA
[b] Department of Neurobiology and Behavior, Cornell University, Ithaca, NY, USA
[c] Department of Biology, Brooklyn College, City University of New York, Brooklyn, NY, USA
[d] Doctoral Subprogram in Ecology, Evolutionary Biology, and Behavior, The Graduate Center, City University of New York, New York, NY, USA
[e] Doctoral Subprogram in Neuroscience, The Graduate Center, City University of New York, New York, NY, USA
[f] Doctoral Subprogram in Behavioral and Cognitive Neuroscience, The Graduate Center, City University of New York, New York, NY, USA
[g] Department of Biology, University of Washington, Seattle, WA, USA
[h] Department of Psychology, University of Washington, Seattle, WA, USA
[i] Virginia Bloedel Hearing Research Center, Seattle, WA, USA

ARTICLE INFO

Keywords:
Acoustic communication
Catecholamines
Dopamine
Noradrenaline
Social decision-making network
Teleost

ABSTRACT

Vocal courtship is vital to the reproductive success of many vertebrates and is therefore a highly-motivated behavioral state. Catecholamines have been shown to play an essential role in the expression and maintenance of motivated vocal behavior, such as the coordination of vocal-motor output in songbirds. However, it is not well-understood if this relationship applies to anamniote vocal species. Using the plainfin midshipman fish model, we tested whether specific catecholaminergic (i.e., dopaminergic and noradrenergic) nuclei and nodes of the social behavior network (SBN) are differentially activated in vocally courting (humming) versus non-humming males. Herein, we demonstrate that tyrosine hydroxylase immunoreactive (TH-ir) neuron number in the noradrenergic locus coeruleus (LC) and induction of cFos (an immediate early gene product and proxy for neural activation) in the preoptic area differentiated humming from non-humming males. Furthermore, we found relationships between activation of the LC and SBN nuclei with the total amount of time that males spent humming, further reinforcing a role for these specific brain regions in the production of motivated reproductive-related vocalizations. Finally, we found that patterns of functional connectivity between catecholaminergic nuclei and nodes of the SBN differed between humming and non-humming males, supporting the notion that adaptive behaviors (such as the expression of advertisement hums) emerge from the interactions between various catecholaminergic nuclei and the SBN.

1. Introduction

Vocal-acoustic social communication is fundamental for reproduction in several vertebrate taxa and is thought to have first evolved in teleost fishes [1]. Furthermore, it has been proposed that social behaviors, including intraspecific vocal communication, are mediated by an evolutionarily conserved assemblage of reciprocally connected hormone-sensitive nuclei located in the basal forebrain and midbrain of

Abbreviations: AT, anterior tuberal hypothalamus; DO/SO, descending and secondary octaval nuclei; IP, isthmal paraventricular nucleus; LC, locus coeruleus; OE, octavolateralis efferent nucleus; PAG, periaqueductal grey; PPa, anterior parvocellular preoptic nucleus; PPp, posterior parvocellular preoptic nucleus; SBN, social behavior network; TH-ir, tyrosine hydroxylase immunoreactivity; TPp, periventricular nucleus of the posterior tuberculum; Vd, dorsal nucleus of the ventral telencephalon; VMN, vocal motor nucleus; VM-VL, ventromedial-ventrolateral thalamic nuclei; Vp, postcommissural nucleus of the ventral telencephalon; VPP, vocal prepacemaker nucleus; VPN, vocal pacemaker nucleus; Vs, supracommisural nucleus of the ventral telencephalon; vT, ventral tuberal hypothalamus; Vv, ventral nucleus of the ventral telencephalon; XL, vagal-associated nuclei.

* Correspondence to: 1301 College Ave, Fredericksburg, VA 22401, USA.
** Correspondence to: 2900 Bedford Ave, Brooklyn, NY 11210, USA.
E-mail addresses: zghahram@umw.edu (Z.N. Ghahramani), pforlano@brooklyn.cuny.edu (P.M. Forlano).

https://doi.org/10.1016/j.bbr.2022.113745
Received 14 July 2021; Received in revised form 28 December 2021; Accepted 11 January 2022
Available online 13 January 2022

all vertebrates, referred to as the "social behavior network" (SBN) [2–5]. Catecholaminergic circuitry, specifically the ascending dopaminergic system and its targets comprising the mesolimbic reward system, is proposed to work in conjunction with the SBN, forming a broader "social decision-making network" (SDMN) in order to assess the salience of socially relevant stimuli and reinforce appropriately adaptive behavioral responses [3,6,7].

Tyrosine hydroxylase (TH) is the rate-limiting enzyme in catecholamine synthesis and TH immunoreactivity (-ir) can be used to demarcate neurons and their fiber projections that produce and release dopamine or noradrenaline, thus resolving potential sites of neuromodulation related to the expression and maintenance of motivated vocal behavior. Notably, previous investigations into the role of catecholamines in coordinating appropriate vocal behavioral expression have focused almost entirely on songbirds. For instance, female European starlings actively engaged in territorial signing had higher levels of phosphorylated (or "activated") TH-ir in the lateral septum (LS) and ventral tegmental area (VTA) compared to silent females [8]. In male European starlings, TH mRNA and dopamine receptor D_1 mRNA expression was correlated with singing behavior in the VTA and Area X (a striatal basal ganglia song nucleus) [9]. It has also been shown that TH-ir neurons in the midbrain periaqueductal grey (PAG) of actively singing male zebra finches showed greater colocalization with the immediate early gene (IEG) ZENK compared to those that remained silent [10]. Moreover, the percentage of TH-ir neurons expressing cFos (a ZENK-like IEG product) in the caudal VTA and central grey (CG) were correlated with the number of songs produced by male zebra finches [11]. In addition to dopamine signaling, noradrenergic activity has been implicated in the modulation of vocal-motor output in male European starlings and zebra finches [12–14]. Relationships have also been shown between ultrasonic vocalization complexity and catecholamine concentrations in the striatum and locus coeruleus (LC) of *Pink1* knockout rats treated with levodopa [15], and a more recent study demonstrated that *Pink1* knockouts possess fewer total LC TH-ir cells compared to wild-type rats [16]. While these findings suggest that catecholamines play an important role in coordinating vocal-motor output in songbirds and potentially in mammals, little is known if this pattern extends to other vocal vertebrates.

The plainfin midshipman fish, *Porichthys notatus*, is an apt model for investigating neural mechanisms that underlie the expression of motivated vocal behavior because production and recognition of social-acoustic signals is key to their reproductive success. Males vocally court females by emitting long-duration advertisement "hums" from under rocky nests in intertidal zones off the northwest coast of the United States during the summer, and females localize males by following their call [17,18]. There are also two distinct reproductive male morphs that possess divergent neuroendocrine profiles and exhibit corresponding alternative mating strategies: type I males are the larger territorial/nesting morph that court females, while the smaller type II males that are incapable of courtship sneak spawn in competition with type Is [19–21].

Midshipman fish possess an expansive vocal-motor neural network with features that are conserved across vocal tetrapods [1,22]. Preoptic and hypothalamic ventral (vT) and anterior (AT) tuberal nuclei are reciprocally connected to the supracommisural (Vs) and ventral (Vv) divisions of the ventral telencelphalon, and project to the midbrain PAG which innervates a rhythmically firing vocal pattern generator (VPG) at the hindbrain-spinal cord boundary [22,23]. The VPG consists of vocal prepacemaker (VPP), pacemaker (VPN) and motor (VMN) nuclei [22, 24–26] and determines the temporal properties of the calls [26]. VMN axons exit the brain via occipital nerve roots to sound-producing vocal muscles attached to the sides of the swim bladder [25] (Fig. 1). Moreover, in a fashion comparable to songbirds [27,28], essential components of the neural circuitry underlying midshipman vocal-acoustic behavior express sex steroid receptors, receive robust catecholaminergic innervation, and overlap considerably with the SBN [2,4,23,29–32] (Fig. 1).

The midshipman vocal control network is rapidly responsive to the exogenous application of steroid hormones, including androgens, estrogens, and glucocorticoids [33,34]. Furthermore, the variation seen in type I male humming behavior during the breeding season has been attributed to differences in glucocorticoid and androgen signaling pathways [35]. Humming type I males possess lower circulating cortisol and higher 11-ketotestosterone (11-KT) compared to non-humming type I males [35], yet the downstream neurochemical targets of these steroids in the brain that integrate social context and expression of humming behavior remain unknown. The catecholaminergic system is an ideal candidate for this function, as androgens have been shown to regulate catecholamine expression and/or correlate with TH-ir neuron number and fiber density in the brains of eels, frogs, songbirds, and mammals [36–39]. It has also been posited that testosterone influences vocal behavior via catecholamine cell groups that project to the forebrain song-control circuit of songbirds [40].

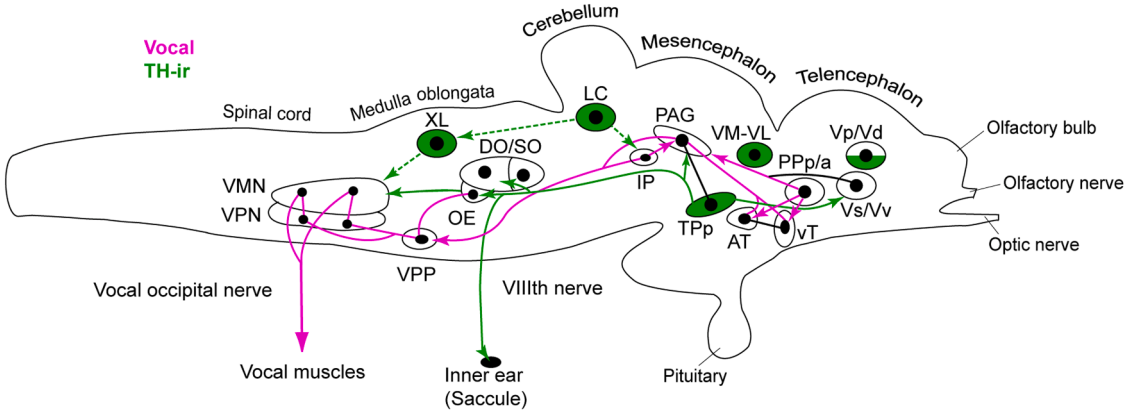

Fig. 1. Schematic sagittal view of the midshipman brain. The vocal-motor system (magenta) receives connections from large TH-ir neurons (green) within the periventricular posterior tuberculum of the diencephalon (TPp). Solid dots represent neurons and lines represent fiber projection pathways. Two connected dots indicate reciprocal connections. Dotted green lines indicate proposed TH-ir connectivity from the locus coeruleus (LC) and vagal-associated nuclei (XL) based on recent neuroanatomical evidence [30,50]. Other abbreviations: V, area ventralis of the telencephalon; Vd, dorsal nucleus of V; Vp, postcommissural nucleus of V; Vs, supracommisural nucleus of V; Vv, ventral nucleus of V; PPa, anterior parvocellular preoptic nucleus; PPp, posterior parvocellular preoptic nucleus; AT, anterior tuberal nucleus; vT, ventral tuberal hypothalamus; VM-VL, ventromedial-ventrolateral thalamic nuclei; PAG, periaqueductal grey; IP, isthmal paraventricular nucleus; DO/SO, descending and secondary octaval nuclei; OE, octavolateralis efferent nucleus; VMN, vocal motor nucleus; VPP, vocal prepacemaker nucleus; VPN, vocal pacemaker nucleus.

Recent immunohistochemical investigations in midshipman have demonstrated immediate early gene (IEG) induction within TH-ir neurons, vocal-acoustic circuitry, and nuclei implicated in social behaviors following playbacks of socially-relevant acoustic stimuli [41–44]. By double-labeling TH-ir neurons with cFos, a commonly utilized IEG protein for measuring neural activation, it was shown that type I male midshipman exposed to conspecific advertisement hums had a greater percentage of TH-ir neurons expressing cFos-ir within the dopaminergic periventricular posterior tuberculum (TPp) and noradrenergic LC compared to ambient noise [44]. Moreover, a complementary study in type II males showed that TH-ir neurons in TPp are selectively activated by advertisement signals and not agonistic grunts [42]. However, no direct associations have been made between TH-ir activity and the production of vocalizations in any non-avian vertebrate.

The goal of this study was to characterize patterns of brain activation between divergent states of calling behavior in type I male midshipman. While previous studies in songbirds have focused on activation of TH-ir neurons within the VTA and PAG during vocalizations [8,10,11], the current study investigated cFos-ir induction within TH-ir neurons in six regions spanning the forebrain and hindbrain (Table 1). It was hypothesized that humming and non-humming type I males would show differences in the expression of cFos-ir within TH-ir neurons adjacent and projecting to vocal circuitry in the hindbrain and throughout the vocal-motor pathway. Quantification of cFos-ir nuclei in TH-ir neurons was carried out in the dorsal (Vd) and postcommissural (Vp) divisions of the ventral telencephalon, ventral thalamic nuclei (VM-VL), TPp, LC, and vagal-associated nuclei (XL) (Fig. 1; Table 1; see [30]). Additionally, cFos-ir neurons were quantified exclusive of TH-ir in several SBN and vocal-acoustic nuclei, such as Vd, Vp, the ventral (Vv) and supracommisural (Vs) divisions of the ventral telencephalon, anterior (PPa) and posterior (PPp) preoptic nuclei, hypothalamic nuclei (vT and AT), and the midbrain PAG (Fig. 1; Table 1). We therefore hypothesized that humming and non-humming type I males would show differences in cFos-ir expression throughout these brain regions of interest. Due to the diverse physiological mechanisms in catecholamine signaling (e.g., mixed inhibition and excitation), there was no a priori reason for a directional hypothesis in this study (e.g., humming males show higher activation in TH-ir neurons or SBN nodes/vocal-acoustic nuclei compared to non-humming males). Since males produce hums that can span minutes to hours [45], we utilized this natural variability in call time to examine which brain regions had cFos-ir most strongly associated with behavioral engagement. It was also hypothesized that correlated activity between TH-ir nuclei and SBN nodes would vary as a function of calling behavior.

Table 1
Catecholaminergic (TH-ir) and social behavior network (SBN)/vocal-acoustic nuclei matched with their corresponding putative mammalian homologues.

Brain area	Putative mammalian homologue
TH-ir	
Vd	Striatum/basal ganglia [89,90,71,91]
Vp	Extended central amygdala/bed nucleus of stria terminalis [4, 92,89,93,63]
VM-VL	Dopaminergic A13 [64,94]
TPp	Dopaminergic A11 [64,94]
LC	Noradrenergic A6 [63,64]
XL	Catecholaminergic A2 [95,96,63,64]
SBN/Vocal-acoustic	
Vv	Septum [22,92,89,93,91]
Vd	Striatum/basal ganglia [89,90,71,91]
Vs	Extended central amygdala/bed nucleus of stria terminalis [4, 92,89,93]
Vp	Extended central amygdala/bed nucleus of stria terminalis [4, 92,89,93]
PPa	Preoptic area [2,97]
PPp	Preoptic area [2,97]
vT	Anterior hypothalamus [2]
AT	Ventromedial hypothalamus (in part) [32, 2, 4]
PAG	Periaqueductal/central gray[2, 22, 4]

2. Methods

2.1. Ethics statement

All experimental animal procedures performed in this study were approved by the Institute for Animal Care and Use Committees of the University of Washington (UW).

2.2. Animals

Fifteen territorial type I male plainfin midshipman fish were hand-collected from nest sites on the Hood Canal, WA during the June-July 2016 and 2017 breeding season and subsequently housed at the Friday Harbor Marine Laboratories on San Juan Island under an ambient light/dark cycle in two 2,000-gallon indoor circular concrete tanks with flow-through seawater that each contained seven artificial nests constructed from cement bricks and granite platters [20,35]. The proximity of the artificial nests was comparable to that found in the field [45]. Ambient temperature was monitored daily and ranged 13–14 °C throughout the course of the experiments, and animals were not fed because nesting males do not eat in the field [46]. Vocal behavior was monitored for 2–3 weeks with individual hydrophones at the entrance of each nest and recorded on a Tascam digital recorder.

Type I male midshipman commence humming soon after nightfall [20,45,47,48]. In this study, all males were initially added to the tank at the same time and after several days of habituation called between 0000 h and 0400 h. After a male stopped humming, the individual was collected from its nest with a net. Non-humming males were collected from the tank at the same time of night when no other males were calling. All humming (n = 9) and non-humming (n = 6) fish were isolated in a bucket for 120 min post-trial and anesthetized by immersion in seawater mixed with 0.025% benzocaine, weighed, measured, and sacrificed via transcardial perfusion with ice-cold teleost Ringer's solution followed by ice-cold 4% paraformaldehyde (Sigma-Aldrich) in 0.1 M phosphate buffer (PB; pH 7.2) [42,44]. Testes were removed and weighed, and gonadosomatic index (GSI) was calculated as the ratio of testes mass to body mass minus testes mass X 100 (Table 2). The size of the testes and vocal muscle verified that all individuals were type I males [20,49]. Brains were dissected, post-fixed for one hour, and transferred to 0.1 M PB. Brains were stored in 0.1 M PB with 0.05% sodium azide until processed. After incubation in 0.1 M PB with 30% sucrose for 48 h, brains were sectioned on the coronal plane at 25 μm with a cryostat and collected in two series onto positively charged slides. One series from each animal was used for this study.

2.3. Immunohistochemistry

Fluorescence immunohistochemistry was slightly modified from a previous protocol [42,44]. Slides were warmed to room temperature prior to being washed 2 × 10 min in 0.1 M phosphate-buffered saline (PBS; pH 7.2), followed by a one-hour soak in blocking solution consisting of 10% normal donkey serum (DS, Jackson ImmunoResearch

Table 2
Summary statistics for morphometric data.

Behavioral state	Humming, n = 9	Non-humming, n = 6
	Range (mean ± SD)	Range (mean ± SD)
Standard length (cm)	13.3–30.0 (21.4 ± 6.1)	15.3–21.2 (18.2 ± 2.3)
Body mass (g)	30.1–449.4 (177.4 ± 152.1)	47.5–147.8 (85.9 ± 37.2)
Gonad weight (g)	0.4–2.9 (1.5 ± 1.0)	0.9–4.1 (1.9 ± 1.2)
GSI (%)[a]	0.5–2.0 (1.1 ± 0.6)	1.4–2.9 (2.2 ± 0.5)

[a] Indicates significant difference between groups ($t_{13} = 3.86$, $p = 0.002$).

Labs, West Grove, PA, USA) + 0.3% Triton X-100 in PBS (PBS-DS-T). After blocking, tissue was incubated for 18 h at room temperature in PBS-DS-T containing mouse anti-TH (1:1000; cat no. MAB318, lot no. 246515; MilliporeSigma, Temecula, CA, USA) and rabbit anti-cFos (1:2000; cat no. sc-253, lot no. C2510; Santa Cruz Biotechnology, Dallas, TX, USA) primary antibodies. After incubation, slides were washed 5 × 10 min in PBS + 0.5% normal donkey serum (PBS-DS), followed by a two-hour incubation in PBS-DS-T combined with anti-mouse and anti-rabbit secondary antibodies conjugated to Alexa Fluor 488 and 568, respectively (1:200; Thermo Fisher Scientific, Waltham, MA, USA). Slides were then washed 3 × 10 min in PBS and coverslipped with ProlongGold containing DAPI nuclear stain (Thermo Fisher). Finally, slides were randomized and coded so that observers were blind to the experimental condition of each animal.

2.4. Image acquisition and anatomy

Images were acquired on an Olympus BX61 epifluorescence compound microscope using MetaMorph imaging and processing software (Molecular Devices, Sunnyvale, CA, USA). Each brain area was imaged with a 20X objective at a constant exposure time and light level. Each image was comprised of consecutively taken photomicrographs using Texas Red, GFP, and DAPI filter sets (Chroma, Bellow Falls, VT, USA) within a z-stack containing 7–10 levels, each with a step of 1 μm (Table S1). All nuclei were sampled unilaterally with the right side of the brain imaged (except TPp, which was sampled bilaterally) in the caudal-to-rostral direction. In the case of tissue loss or damage, the opposite side of the brain was used or the section was omitted. As a way of determining confidence in cell count estimates, an animal was excluded from the analysis if it was missing more than half the average number of sections sampled per subject for a given brain area, explaining the exclusion of two humming males in the XL analysis (Tables 3–4).

Catecholaminergic nuclei of interest included Vd, Vp, VM-VL, TPp, LC, and XL (Table 1). Sampling of TH-ir neurons was done as previously described [29,41,42,44,50]. Activation of these nuclei was measured by the occurrence of a cFos-ir nucleus within a TH-ir neuron, referred to herein as colocalization [11,41,42,44,51]. Individual TH-ir neurons were counted only if the perimeter of the cell was clearly outlined with a labeled neurite in addition to having a nucleus that showed colocalization with DAPI. The sum of TH-ir neurons containing cFos-ir was divided by the total number of TH-ir neurons X 100 for a percentage of TH+cFos-ir colocalization. There were no differences between humming and non-humming males in numbers of sections sampled for any TH-ir nuclei (unpaired t-test, $p > 0.1$ in all cases) (Table S1).

SBN and vocal-acoustic nuclei analyzed for the presence of cFos-ir exclusive of TH-ir included Vv, Vd, Vs, Vp, PPa, PPp, vT, AT, and PAG (Table 1). Sampling of these nuclei was carried out as previously described [29,41,42,44,50]. Quantification of DAPI-labeled cell nuclei containing cFos-ir signal was carried out using a custom-written macro in ImageJ (NIH, USA) [41,42,52]. The average number of cFos-ir cells per section (total number of cFos-ir cells divided by total number of sections sampled) was then calculated per brain region in each animal. There were no differences in numbers of sections sampled for any SBN and vocal-acoustic nuclei (unpaired t-test, $p > 0.1$ in all cases) (Table S1).

Table 3
Descriptive statistics for comparison of cFos induction across catecholaminergic (TH-ir) nuclei of interest between humming and non-humming males.

%TH+cFos-ir	Condition	Min	Max	Mean	SD
Vd	Humming (n = 9)	0.0	4.4	2.3	1.4
	Non-humming (n = 6)	0.9	2.5	1.7	0.6
Vp	Humming (n = 9)	0.0	14.7	4.6	4.9
	Non-humming (n = 6)	1.3	5.8	3.5	1.7
VM-VL	Humming (n = 9)	0.0	2.7	1.4	0.8
	Non-humming (n = 6)	0.8	3.2	1.8	1.0
TPp	Humming (n = 9)	0.9	14.8	3.7	4.4
	Non-humming (n = 6)	0.0	4.8	2.0	2.1
LC	Humming (n = 9)	2.2	44.2	20.5	14.5
	Non-humming (n = 6)	5.6	41.4	21.0	14.2
XL (para)	Humming (n = 7)	0.0	50.0	22.8	19.7
	Non-humming (n = 6)	0.0	50.0	19.0	18.6
XL (extra)	Humming (n = 7)	36.2	74.4	55.2	12.6
	Non-humming (n = 6)	29.6	71.8	49.3	15.9
XL (all)	Humming (n = 8)	9.8	73.9	48.0	19.3
	Non-humming (n = 6)	28.6	69.1	47.6	15.0

Table 4
Descriptive statistics for comparison of total catecholaminergic (TH-ir) cell counts between humming and non-humming males.

TH-ir neurons	Condition	Min	Max	Mean	SD
Vd	Humming (n = 9)	169.0	327.0	248.9	55.4
	Non-humming (n = 6)	151.0	334.0	254.0	67.4
Vp	Humming (n = 9)	36.0	92.0	65.8	19.5
	Non-humming (n = 6)	52.0	79.0	64.2	11.8
VM-VL	Humming (n = 9)	219.0	404.0	310.7	52.3
	Non-humming (n = 6)	218.0	394.0	303.2	64.2
TPp	Humming (n = 9)	196.0	362.0	286.8	54.8
	Non-humming (n = 6)	229.0	319.0	270.0	33.4
LC[a]	Humming (n = 9)	37.0	67.0	48.3	10.8
	Non-humming (n = 6)	29.0	42.0	36.8	4.9
XL (para)	Humming (n = 7)	1.0	9.0	4.6	2.5
	Non-humming (n = 6)	0.0	10.0	5.2	3.9
XL (extra)	Humming (n = 7)	58.0	106.0	76.3	18.7
	Non-humming (n = 6)	54.0	77.0	61.5	10.0
XL (all)	Humming (n = 8)	59.0	112.0	78.4	19.6
	Non-humming (n = 6)	57.0	83.0	66.7	12.1

[a] Indicates significant difference between groups ($t_{13} = 2.43$, $p = 0.031$).

2.5. Statistics

Statistical analyses were performed at the $\alpha = 0.05$ significance level using GraphPad Prism version 7 (La Jolla, CA, USA). Data for % TH+cFos-ir (Vd, Vp, VM-VL, TPp, LC, XL) and cFos-ir/section (Vv, Vd, Vs, Vp, PPa, PPp, vT, AT, PAG) were analyzed using unpaired t-tests with divergent behavioral states (humming and non-humming) as independent groups of comparison. Shapiro-Wilk tests were used to assess normality and a Mann-Whitney U test was used to compare mean ranks if the data violated Gaussian assumptions. A Welch-corrected t-test was used if the result of an F-test showed significant heterogeneity of variance between groups. Data for fish in each group were then pooled and two separate Pearson correlation matrices were computed between all nuclei of interest to investigate functional relationships between cFos-ir colocalizaiton within TH-ir nuclei and cFos-ir response within SBN nodes as a function of the behavioral state of the animal. To control for multiple comparisons within the same dataset, p-values were adjusted using the Benjamini-Hochberg correction [53] with a false discovery rate (FDR) of 0.25 [41,42,54]. A subset of significant correlations did not remain after correction and are indicated as such (Tables S2-S3). Networks formed among TH-ir nuclei and SBN nodes were characterized with UCINET version 6.7 [55] using density as a measure of cohesion and eigenvalues as a measure of centrality [56]. Density measures the degree to which all nodes of a network interact with all other nodes. Eigenvalue centrality takes into account not only how well a node is connected (degree centrality), but also how well-connected each of its connected nodes are. This measure of centrality emphasizes that, all else being equal, an individual node is more likely to play a key role in information processing when its immediate connections are well connected themselves. Network density was compared between groups using a t-test bootstrapped to 5000 subsamples. The Quadratic Assignment Procedure (QAP) was utilized with 5000 permutations to test for shifts in functional connectivity among network nodes between humming and non-humming males. The QAP is similar to a Mantel test [57]. First, a standard regression is calculated across all corresponding

correlation coefficients (e.g., r-values) for each pair of networks to be tested (e.g., humming and non-humming). The r-values of one matrix are then randomly rearranged and the regression is repeated. This permutation process is repeated 5000 times and the observed regression coefficient is compared to the distribution of coefficients in order to determine a p-value. The null hypothesis under QAP entails no association between the two matrices being compared, hence an insignificant p-value indicates that they are different [42,57–60]. Networks were visualized with undirected graphs using the Fruchterman-Reingold algorithm in Gephi 0.9.3 [61]. Statistics are reported as mean ± standard error (SEM) unless otherwise noted. All p-values reported are two-tailed.

3. Results

Morphological analyses were performed on all humming (n = 9) and non-humming (n = 6) fish used in this study. See Table 2 for a complete breakdown of standard length (SL), body mass (BM), gonad weight (GW), and gonadosomatic index (GSI). There were no differences in SL (Welch-corrected $t_{10.92} = 1.41$, $p = 0.186$), BM (Welch-corrected $t_{9.38} = 1.73$, $p = 0.117$), or GW ($t_{13} = 0.75$, $p = 0.47$) between humming and non-humming males. However, investment in testes as a proportion of body mass (GSI) was 66.7% greater in non-humming males ($t_{13} = 3.86$, $p = 0.002$; humming = 1.1 ± 0.2% and non-humming = 2.2 ± 0.2%) (Table 2). Within the group of humming males, total hum duration ranged from 1.4 to 30.6 min (Fig. 2). Most fish produced 1–2 hums approximately 150 min prior to anesthesia except for the instance where one fish produced six short-duration hums over 3.5 h, the last of which occurred 120 min prior to anesthesia (Fig. 2). This animal was included in the analysis because there was no correlation between time to anesthesia and total hum duration ($p > 0.6$) or any cFos-ir measures in the current study ($p > 0.6$ in all cases). Additionally, it has been shown that induction of cFos protein levels in the brains of medaka fish remained elevated for up to 150 min [62].

3.1. Activation of TH-ir neurons

There were no differences in %TH+cFos-ir neurons between humming and non-humming males in Vd ($t_{13} = 1.1$, $p = 0.308$), Vp (Welch-corrected $t_{10.6} = 0.62$, $p = 0.546$), VM-VL ($t_{13} = 0.79$, $p = 0.443$), TPp ($U = 18$, $p = 0.313$), LC ($t_{13} = 0.1$, $p = 0.949$), XL ($t_{12} = 0.04$, $p = 0.966$), or the paraventricular ($t_{11} = 0.35$, $p = 0.747$) and extra-ventricular ($t_{11} = 0.75$, $p = 0.467$) XL subgroups (Fig. 3A; Table 3). However, with regard to total TH-ir neurons (exclusive of cFos-ir), humming males had 27% more in the LC compared to non-humming males ($t_{13} = 2.43$, $p = 0.031$; humming = 48.3 ± 3.6 and non-

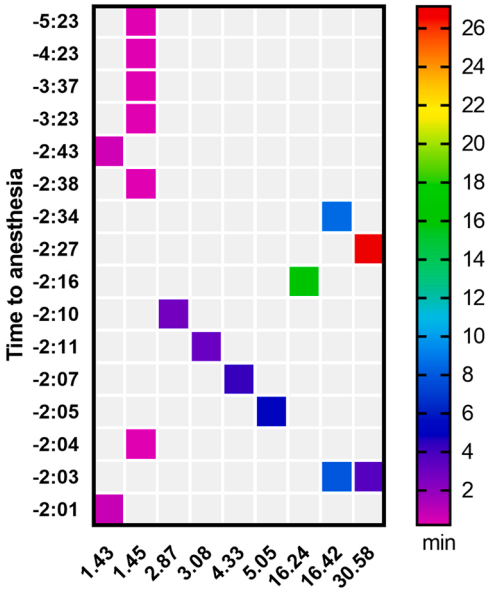

Fig. 2. Summary of humming male behavioral data. Columns in the vocal actogram represent individual fish ordered from shortest to longest total hum duration, and colored squares represent individual hums of variable duration that occurred t-minus x-hours: x-minutes prior to anesthetizing the animal.

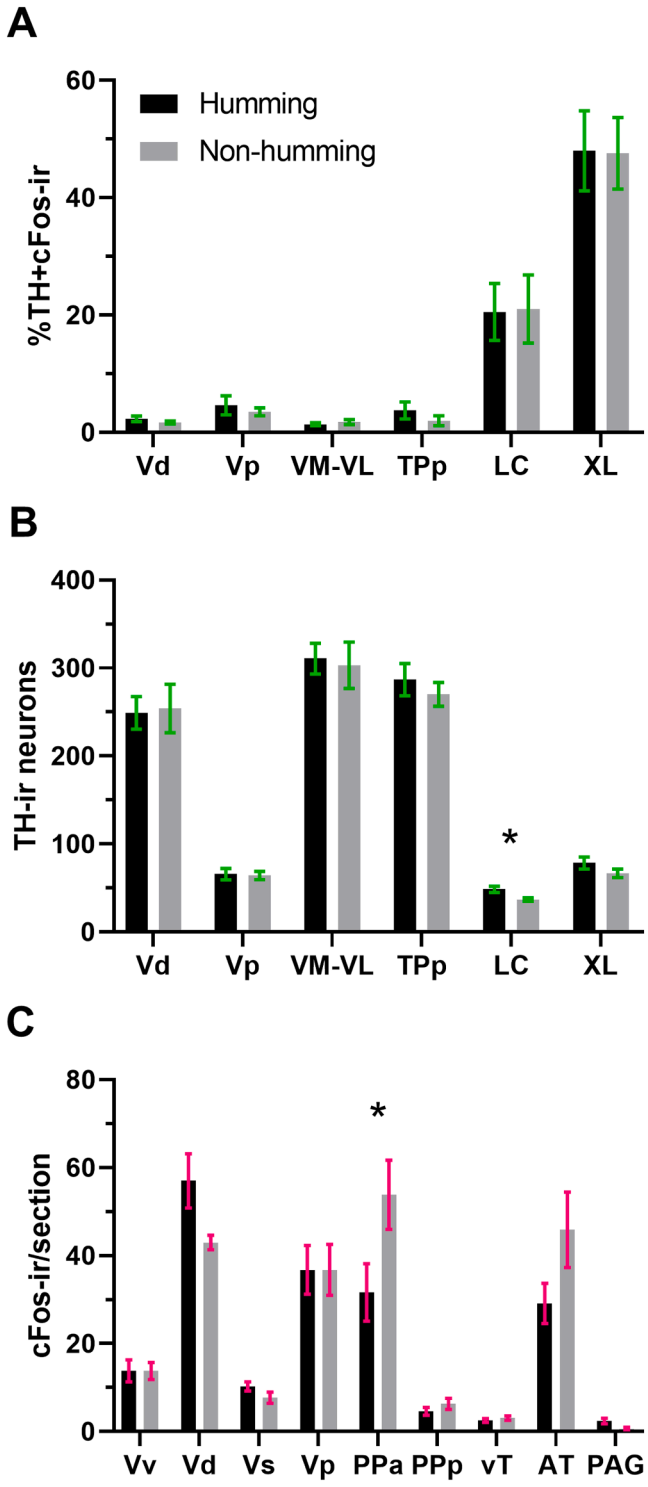

Fig. 3. cFos induction across catecholaminergic and SBN nuclei of interest. Percentage of TH+cFos-ir colocalization (A) and TH-ir cell counts (B) within catecholaminergic nuclei and cFos-ir cells/section (C) within SBN nuclei in humming and non-humming males. Error bars represent mean ± SEM. *Indicates significant difference between groups ($p \leq 0.036$).

humming = 36.8 ± 2.0) (Fig. 3B; Fig. 4B; Table 4). Otherwise, there were no differences in total TH-ir neurons between groups in Vd (t_{13} = 0.16, p = 0.875), Vp (t_{13} = 0.18, p = 0.859), VM-VL (t_{13} = 0.25, p = 0.807), TPp (t_{13} = 0.67, p = 0.517), XL (t_{12} = 1.29, p = 0.223), or the paraventricular (t_{11} = 0.33, p = 0.747) and extraventricular (t_{11} = 1.73, p = 0.112) XL subgroups (Fig. 3B; Table 4).

3.2. Activation of SBN and vocal-acoustic nuclei

Non-humming males had significantly more cFos-ir neurons/section in the PPa compared to humming males (U = 9, p = 0.036; humming male mean rank = 6 and non-humming male mean rank = 11) (Fig. 3C; Table 5). Otherwise, there were no differences in cFos-ir neurons/section between groups in Vv (t_{13} = 0.01, p = 0.995), Vs (t_{13} = 1.58, p = 0.137), Vp (t_{13} <0.01, p = 0.999), PPp (t_{13} = 1.15, p = 0.272), vT (t_{13} = 0.794, p = 0.441), or AT (U = 14, p = 0.145), although there were trending differences toward humming males having more cFos-ir/section in Vd (Welch-corrected $t_{9.1}$ = 2.2, p = 0.055) (Fig. 5E) and PAG (t_{13} = 2.16, p = 0.05) (Fig. 5H).

3.3. Relationships between hum duration and activation of TH-ir/SBN nuclei

Within the group of humming males (n = 9), Pearson correlations revealed several significant positive relationships between total hum duration (ranging from 1.4 to 30.6 min) and cFos-ir induction in TH-ir and SBN nuclei (Table 6). Specifically, there were significant correlations between total hum duration and %TH+cFos-ir in LC (r = 0.928, p < 0.001) (Fig. 4C), and cFos-ir/section in Vv (r = 0.7, p = 0.036) (Fig. 5C), Vd (r = 0.906, p < 0.001) (Fig. 5F), and PAG (r = 0.863, p = 0.003) (Fig. 5I).

3.4. Coactivation of TH-ir neurons with SBN nuclei

Pairwise Pearson correlation matrices were constructed to examine differences in functional connectivity between TH-ir and SBN nuclei in humming and non-humming type I males. Each behavioral state had correspondingly different sets of significant correlations among network nodes (Fig. 6; Tables S2-S3), supporting distinct patterns of co-activation underlying the expression of advertisement hums. Interestingly, non-humming males showed strong co-activation between %TH+cFos-ir in the LC and XL (r = 0.955, p = 0.003) (Fig. 6B; Table S2), and this relationship persisted within the putatively noradrenergic extraventricular vagal subgroup [50] (r = 0.963, p = 0.002).

Table 5
Descriptive statistics for comparison of cFos induction across SBN nuclei of interest between humming and non-humming males.

cFos-ir/section	Condition	Min	Max	Mean	SD
Vv	Humming (n = 9)	2.0	23.7	13.8	7.5
	Non-humming (n = 6)	7.5	18.8	13.8	4.8
Vd	Humming (n = 9)	37.3	93.7	57.0	18.5
	Non-humming (n = 6)	37.1	47.8	43.0	4.0
Vs	Humming (n = 9)	6.3	16.0	10.2	3.1
	Non-humming (n = 6)	3.6	11.1	7.7	3.1
Vp	Humming (n = 9)	11.5	63.3	36.8	16.6
	Non-humming (n = 6)	22.8	62.6	36.8	14.1
PPa[a]	Humming (n = 9)	14.9	70.2	31.6	19.5
	Non-humming (n = 6)	25.6	71.2	53.9	19.3
PPp	Humming (n = 9)	1.5	10.2	4.6	2.7
	Non-humming (n = 6)	3.4	11.4	6.3	3.1
vT	Humming (n = 9)	1.0	5.0	2.5	1.3
	Non-humming (n = 6)	1.5	4.7	3.1	1.3
AT	Humming (n = 9)	6.7	53.0	29.1	13.8
	Non-humming (n = 6)	28.7	74.3	45.9	21.0
PAG	Humming (n = 9)	0.0	5.5	2.4	1.9
	Non-humming (n = 6)	0.0	1.8	0.6	0.8

[a] Indicates significant difference between groups (U = 9, p = 0.036).

The Quadratic Assignment Procedure (QAP) was used to statistically compare random permutations of the correlation matrices formed among network nodes, thereby testing for differences in functional connectivity between behavioral states. The results of the QAP detected no similarity in patterns of brain activation between humming and non-humming males (r = −0.025, p = 0.482) (Fig. 6; Fig. S1; Tables S2-S3), and there was no difference in overall network density between the two groups (t = 0.099, p = 0.922) (Table 7). However, regarding network centrality, divergent states of vocal behavior showed differential recruitment of TH-ir and SBN nuclei: within humming males, LC showed the highest recruitment among TH-ir nuclei, and Vv, Vd, Vs, and PAG showed the highest recruitment among SBN nodes (Table 7). In the group of non-humming males, Vd showed the highest recruitment among TH-ir nuclei, and Vs, vT, and AT showed similarly high centrality scores among SBN nodes (Table 7).

4. Discussion

This study provides novel insight into catecholaminergic and SBN activation during the behavioral state of vocal courtship in a teleost. While there was only one significant difference between humming and non-humming males in the expression of cFos-ir within the PPa, the PAG

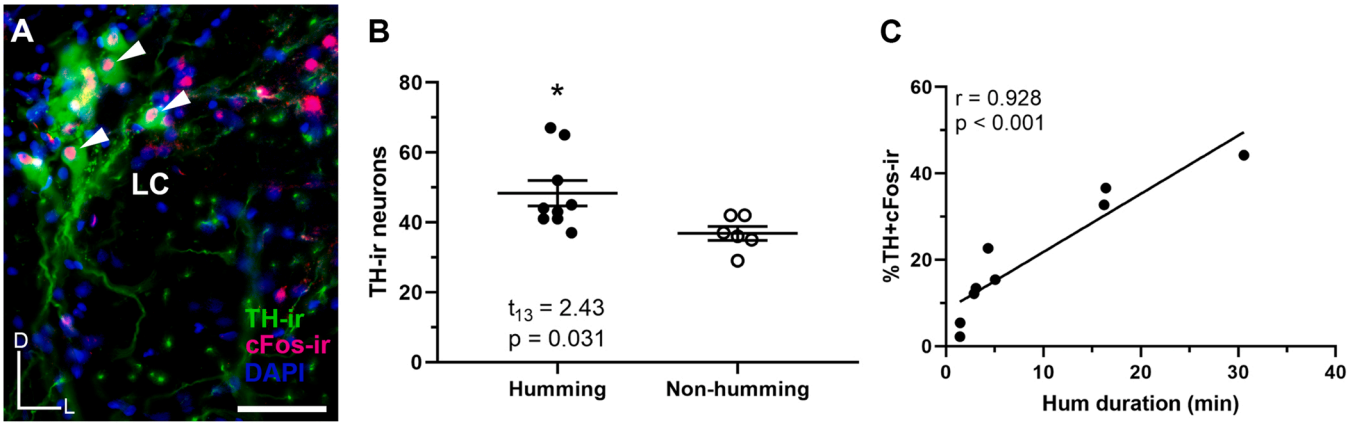

Fig. 4. TH-ir neuron number in the locus coeruleus (LC) differentiates humming from non-humming males and percent TH+cFos-ir colocalization reflects call duration. Arrows indicate cFos-ir (red) colocalized to TH-ir (green) neurons in a representative image (A) of the noradrenergic LC in a humming male. Compass in the bottom left corner of (A) represents the dorsal (D) and lateral (L) orientation of the image. Scale bar = 100 μm. Graph in (B) shows a comparison of TH-ir neuron number between humming and non-humming males; error bars represent mean ± SEM. Graph in (C) depicts percent TH+cFos-ir colocalization in the LC scaled to total hum duration.

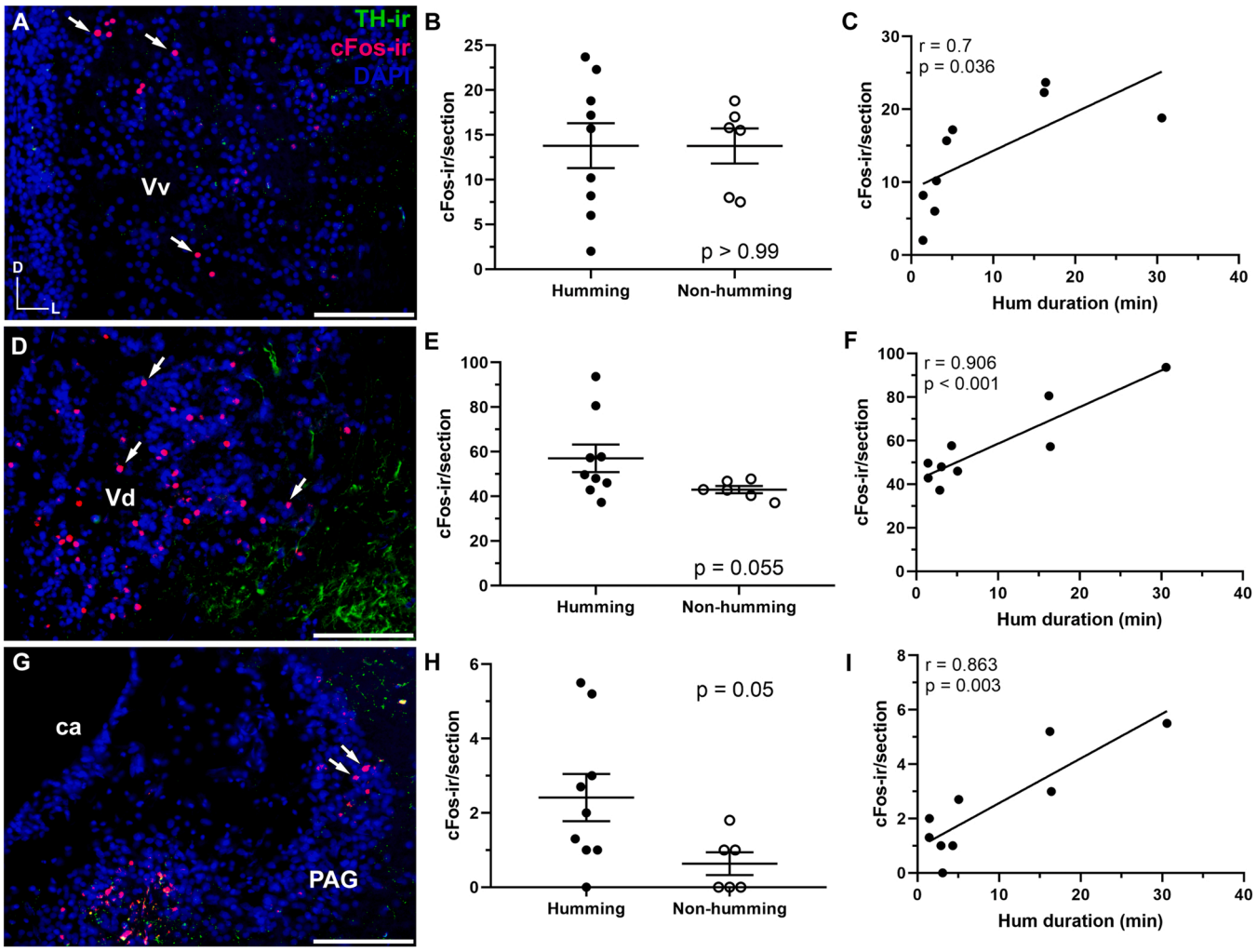

Fig. 5. Activation of SBN nuclei reflects call duration. Representative images (A, D, G) of cFos-ir neurons (red) within the ventral division of the ventral telencephalon (Vv; A), dorsal division of the ventral telencephalon (Vd; D), and periaqueductal grey (PAG; G) in humming males. Compass in the bottom left corner of (A) represents the dorsal (D) and lateral (L) orientation for each image. Scale bars = 100 μm. ca = cerebral aqueduct. Graphs (B, E, H) show a comparison of cFos-ir/section in SBN nodes Vv (B), Vd (E), and PAG (H) between humming and non-humming males; error bars represent mean ± SEM. Graphs (C, F, I) depict mean cFos-ir/section in Vv (C), Vd (F), and PAG (**I**) scaled to total hum duration.

Table 6
Correlations between the total amount of time males spent humming and percentage of TH+cFos-ir colocalization in catecholaminergic nuclei and cFos-ir/section in SBN nuclei.

	r	95% CI	p
%TH+cFos-ir			
Vd	0.363	[− 0.397, 0.827]	0.338
Vp	0.634	[− 0.052, 0.914]	0.067
VM-VL	0.159	[− 0.565, 0.745]	0.682
TPp	0.429	[− 0.329, 0.851]	0.250
LC[a]	0.928	[0.686, 0.985]	< 0.001
XL	0.033	[− 0.688, 0.721]	0.938
cFos-ir/section			
Vv[a]	0.700	[0.066, 0.931]	0.036
Vd[a]	0.906	[0.608, 0.980]	< 0.001
Vs	0.587	[− 0.127, 0.900]	0.097
Vp	0.596	[− 0.113, 0.903]	0.090
PPa	0.018	[− 0.654, 0.674]	0.964
PPp	0.121	[− 0.591, 0.727]	0.757
vT	0.627	[− 0.064, 0.912]	0.071
AT	0.397	[− 0.363, 0.840]	0.290
PAG[a]	0.863	[0.466, 0.971]	0.003

[a] Indicates significant correlation with total hum duration at $p < 0.05$.

(a known vocal node in the midbrain) and Vd (striatal homologue) were both near the threshold for significance. While the large variation in duration of humming behavior (~1–30 min) may explain some of the minimal differences measured between groups, few differences in cFos induction of individual nuclei between humming and non-humming groups is not unexpected. The nuclei sampled presumably contain only a subset of neurons connected to and influencing the descending vocal motor pathway; these nuclei likely serve social, homeostatic, or locomotor functions as well [2]. Catecholaminergic nuclei are likely even more extreme in the diversity of their function and wide-ranging projection patterns of individual neurons [63–65]. All of this further supports the value of using network analyses when comparing different behavioral states and the importance of measuring changes in individual nuclei within the humming group as a function of increased behavior [66]. It is also possible that cells may be physiologically active without expressing cFos under our particular sampling protocol. Furthermore, many non-catecholaminergic nuclei measured in this study (e.g., ventral telencephalon, preoptic area, hypothalamus, PAG) consist of a mix of inhibitory (GABAergic) and excitatory neurons [67,68] that would not be discernible by cFos-ir alone and therefore different behavioral states may have similar numbers but different subtypes of activated neurons. It is also possible that induction of cFos-ir in these nuclei may be context-dependent in that they require exposure to certain

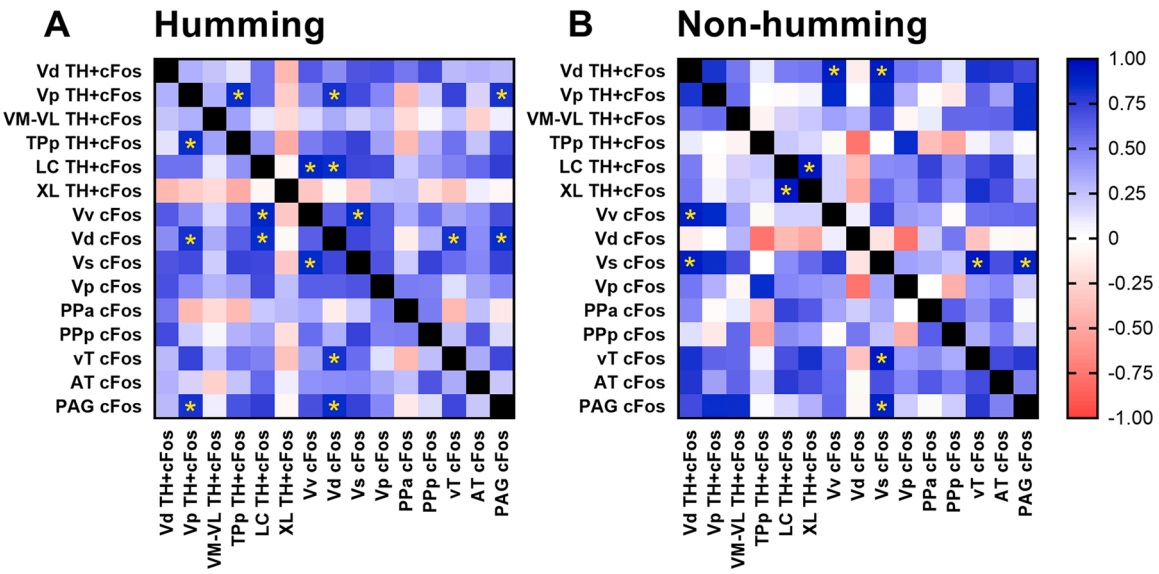

Fig. 6. Patterns of correlated activity among TH-ir and SBN nuclei differ as a function of behavioral state. Heatmap matrices represent pairwise Pearson correlations between TH-ir nuclei and SBN nodes (boxes) in humming (A) and non-humming (B) males. Colors indicate correlation coefficients (r-values) and gold asterisks (*) denote significant correlations after adjusting for multiple comparisons ($p \leq 0.015$; see Tables S2-S3). Black boxes are self-correlations ($r = 1$); data are mirrored above and below the diagonal.

Table 7
Characterization of the SBN for each behavioral state using cFos-ir induction as a marker of neuronal activity.

		Humming	Non-humming
Density		0.346	0.337
Eigenvector	**TH+cFos**		
	Vd	0.246	**0.353**
	Vp	0.296	0.259
	VM-VL	0.109	0.242
	TPp	0.272	0.046
	LC	**0.320**	0.253
	XL	-0.107	0.271
	cFos		
	Vv	**0.315**	0.275
	Vd	**0.333**	-0.079
	Vs	**0.350**	**0.357**
	Vp	0.266	0.185
	PPa	0.033	0.190
	PPp	0.225	0.124
	vT	0.259	**0.353**
	AT	0.195	**0.325**
	PAG	**0.304**	0.291

Reported values correspond to network cohesion (density) and centrality (eigenvalue) of each brain region. Bold eigenvalues indicate high levels of centrality (>0.3) among network nodes.

social/environmental stimuli before showing detectable levels of activation. As such, the absence of elevated cFos protein expression does not imply that those brain regions are not involved in midshipman advertisement calling.

Several elegant papers have delineated the descending vocal motor circuitry in midshipman via tract tracing combined with electrical stimulation [22,69,70], so while vocal circuitry in midshipman has been defined for some time (many of which overlap with the SBN [2]), a visualization of the activation pattern of multiple vocal-motor nodes during sustained courtship vocalization was previously unknown. Importantly, the large range of individual humming behavior observed in the current study offered an additional and important variable to understand activation of specific nuclei as a function of advertisement call duration. There indeed were significant positive relationships between the total amount of time males spent humming and %TH+cFos-ir in LC and cFos-ir/section in Vv, Vd, and PAG. It was also determined that divergent states of calling behavior engendered shifts in functional connectivity between TH-ir and SBN nuclei, suggesting that the two circuits form a network that could arbitrate variation in humming behavior within type I males during the breeding season (see below).

Noradrenergic neurons in the LC are appropriate candidates for integrating sensory-motor processes in midshipman, as they appear to send ascending projections to higher-order midbrain and forebrain processing centers [30,64,71]. It has been shown that LC TH-ir neurons are responsive to playbacks of conspecific advertisement hums in type I males [44], directly implicating this nucleus in auditory-driven social behaviors. The current study is the first to link noradrenergic activity in the LC with the expression of courtship vocalizations in midshipman, as humming type I males had more TH-ir neurons in this region compared to non-humming males, and LC TH+cFos-ir colocalization was positively correlated with total hum duration (ranging from 1.4 to 30.6 min). Using EGR-1 (ZENK) as a marker of neural activation, previous studies in two different species of songbirds did not show induction of noradrenergic neurons in LC during male singing [10,72]. However, a recent study in male zebra finches demonstrated a direct role for noradrenaline on switching cortical motor output from undirected to directed song [14]. Additionally, in male zebra finches, chemical lesioning of noradrenergic neurons caused an increase in latency to sing [73], and abolished context-dependent motor-driven gene expression in Area X (a songbird basal ganglia nucleus) [27]. Interestingly, it was recently determined that *Pink1* knockout rats (a genetic model of early-onset Parkinson's Disease) have significant vocal impairments and fewer total LC TH-ir cells when compared to wild-type rats [16] and treatment with noradrenergic reuptake inhibitor improves vocalization measures [74]. Hence, noradrenergic LC neurons could similarly mediate the effects of environmental context on arousal and humming behavior in midshipman.

The current study is the first to establish relationships between advertisement calling in midshipman and cFos-ir induction within specific SBN nodes, as activity in Vv, Vd, and PAG was positively correlated with total hum duration (there was also a trend toward humming males having more cFos-ir in Vd and PAG). These findings are corroborated by the fact that vocal-motor activity is readily evoked via electrical stimulation of vT, AT, and PAG [69,70,75–77], and ventral telencephalic nuclei (e.g., Vv, Vd) are reciprocally connected with the forebrain

vocal-acoustic complex, including AT [22,70]. Furthermore, both vT and AT send projections to PAG [70]. Since midshipman tend to possess very few PAG TH-ir neurons [30], quantifying TH+cFos-ir colocalization in this region was not feasible in the current study. It is interesting to note that EGR-1 induction within TH-ir neurons in the PAG differentiated singing from silent male zebra finches but was not correlated with the amount of singing produced, suggesting that PAG TH-ir neurons are involved in motivational or attentional aspects of vocalization rather than vocal motor output [10]. However, the current findings in midshipman suggest that activation of the PAG is more directly involved in vocal motor output, as cFos-ir induction in this nucleus was positively correlated with hum duration. This is consistent with studies showing PAG as a prominent area for eliciting fictive vocalizations via brain stimulation [22,69,70,78]. Moreover, a recent study in midshipman found that humming type I males exhibited greater ps6 activation of isotocin receptor containing neurons in the PAG compared to non-humming males [79].

Non-humming males exhibited significantly more cFos-ir induction in the PPa compared to humming males. Fictive vocal-motor responses obtained from electrical stimulation of vT are inhibited by the neuropeptides arginine vasotocin and isotocin, homologs of vasopressin and oxytocin, respectively, which are produced for central, nonhypophysial release by the PPa [75,77]. Given that the PPa sends vasotonergic and isotonergic projections to all components of the midbrain and forebrain vocal-acoustic complexes in midshipman [77,80], it is possible that greater induction of cFos-ir in the PPa of non-humming males observed in the current study is reflective of parvocellular preoptic inhibitory function on vocal behavior; however, double-labeling cFos with non-apeptide antibodies would be needed to support this explanation. A recent study in midshipman using RNA-sequencing showed differential gene expression between humming and non-humming type I males in the preoptic area-anterior hypothalamus (POA-AH) [81], an area that includes PPa. Another recent study also found that humming males showed greater ps6 activation of neurons expressing isotocin receptors in the PPa compared to non-humming males [79].

Correlation matrices were created to visualize coactivation of TH-ir nuclei with SBN nodes, and to resolve shifts in functional connectivity that could be attributed to differences in behavior between humming and non-humming type I males. After adjusting p-values to account for multiple comparisons, 13 out of 33 significant correlations remained as such (see Tables S2-S3). Therefore, caution should be exercised when interpreting these results as they could represent false positives given the large number of tests run (210 in total). However, those higher p-values (e.g., $\geq$0.018) which were no longer significant after correction may be attributed to low power due to small sample sizes rather than being random and spurious [82]. Dopaminergic neurons in Vp and TPp were co-active in males that were actively humming, and both of these nuclei showed correlated activity in type II male midshipman that were exposed to hums of type I males [42], suggesting that both nuclei play an important role in the production and perception of advertisement calls. Humming males also showed correlated activity between dopaminergic activity in Vp with cFos-ir induction in Vd and PAG, suggesting that dopaminergic input to these SBN nodes influences the expression of advertisement calls. In non-humming males, dopaminergic activity in Vd was correlated with cFos-ir induction in Vv and Vs, suggesting local ventral telencephalic influence of dopaminergic signaling in the absence of advertisement calling. The TH-ir neurons in TPp are particularly well-positioned to modulate vocal behavior, as a reciprocal connection between PAG and TPp nuclei has been previously demonstrated [70]. Dopaminergic TPp neurons appear to project directly to the ventral telencephalon (Vs, Vv), PAG, and the vocal pattern generator in the hindbrain-spinal cord [30] and lie in an area replete with androgen [31], estrogen [32,83], aromatase [32,84] and melatonin 1b receptor expression [85] and are therefore likely downstream targets of circulating 11-KT, melatonin, and locally-produced estrogen, all well documented modulators of increased vocal output and excitability in type I males [18,33,86].

In humming males, TH-ir activity in LC was correlated with cFos-ir induction in Vv and Vd, whereas in non-humming males there was a correlation between TH-ir activity in LC and XL. A previous neuroanatomical study found that type II male midshipman possess more extraventricular vagal TH-ir neurons in parallel proximity to the VMN compared to type I males during the breeding season [50]. Therefore, the co-activation of LC and XL TH-ir neurons observed in the current study could be related to a network involved in the suppression of humming behavior within the type I male morphotype. The causal relationship of LC and XL activity to humming behavior is an important area for future experimental studies. There were also some notable shifts in relationships among the SBN/vocal-acoustic nuclei, as humming males showed correlations between cFos-ir in Vv with vT and PAG, whereas in non-humming males both vT and PAG were correlated with Vs (Fig. 6; Fig S1; Tables S2-S3). It is therefore possible that shifts in correlated activity between vocal-acoustic circuitry (vT, PAG) and the ventral telencephalon (Vv, Vs) provide another substrate for divergent vocal behavioral states in midshipman.

Humming and non-humming males showed some overlap and differences in network recruitment of TH-ir and SBN nuclei. For example, cFos-ir in Vs showed similar centrality scores irrespective of the behavioral state of the animal, suggesting that it may act as a central control hub in the network. However, humming males showed high recruitment of TH-ir neurons in LC as well as cFos-ir in Vv, Vd, and PAG, whereas non-humming males showed high recruitment of TH-ir neurons in Vd and cFos-ir in vT and AT. Importantly, the isthmal paraventricular nucleus (IP) sends afferent projections to the PAG and appears to receive significant noradrenergic input from the LC [22,30,70,87,88] (see Fig. 1). Furthermore, the midbrain vocal-acoustic complex (including PAG and IP) is reciprocally connected with the forebrain vocal-acoustic complex (e.g., vT, AT), which in turn is reciprocally connected with the ventral telencephalon (e.g., Vv, Vd) [22,70]. Therefore, the expression of advertisement hums may be contingent upon contemporaneous signaling between vocal-acoustic circuitry and these hindbrain noradrenergic and ventral telencephalic nuclei. Intriguingly, XL TH-ir neurons showed a negative eigenvalue (−0.107) within the humming male network, and a positive eigenvalue (0.271) in the non-humming male network (see Table 7), further suggesting that recruitment of vagal-associated neurons may inhibit humming behavior within type I males.

4.1. Conclusion

In conclusion, it was determined that the number of TH-ir neurons in the noradrenergic LC and cFos-ir induction in the preoptic area (PPa) differentiated humming from non-humming type I male midshipman. Within humming males, cFos-ir induction in LC TH-ir neurons and in ventral forebrain (Vv, Vd) and midbrain (PAG) SBN nuclei were positively correlated with the total amount of time spent humming. These results assert an important role for specific catecholaminergic brain regions in the production of motivated reproductive-related vocalizations. Divergent states of humming behavior also evoked correspondingly distinct shifts in functional connectivity among TH-ir and SBN nuclei, supporting the idea that adaptive behaviors such as the expression of advertisement hums emerge from the interactions between the various catecholaminergic nuclei and SBN.

Funding

This study was supported by funds from the PADI Foundation grant #14931 and the Lerner Gray Memorial Fund of the American Museum of Natural History (to Zachary N. Ghahramani), NSF IOS 1456700 (to Joseph A. Sisneros), and NSF IOS 1456743 (to Paul M. Forlano).

CRediT authorship contribution statement

Zachary Ghahramani: Conceptualization, Methodology, Software, Validation, Formal analysis, Investigation, Data curation, Writing – original draft, Visualization, Supervision, Project administration, Funding acquisition. **Jonathan Perelmuter:** Investigation, Writing – review & editing. **Joshua Varughese:** Software, Formal analysis, Data curation. **Phoo Kyaw:** Software, Formal analysis, Data curation. **William Palmer:** Formal analysis, Investigation, Data curation. **Joseph Sisneros:** Conceptualization, Methodology, Investigation, Resources, Writing – review & editing, Supervision, Project administration, Funding acquisition. **Paul Forlano:** Conceptualization, Methodology, Investigation, Resources, Writing – review & editing, Visualization, Supervision, Project administration, Funding acquisition.

Declaration of Competing Interest

The authors wish to declare no conflicts of interest.

Acknowledgements

We wish to thank the UW Friday Harbor Marine Lab and Orphal Colleye for logistical support as well as Chris Braun, Thomas Preuss, and Andy Bass for granting constructive critique on an earlier version of this manuscript. We also thank the anonymous reviewers whose comments greatly improved the quality of the manuscript.

Appendix A. Supporting information

Supplementary data associated with this article can be found in the online version at doi:10.1016/j.bbr.2022.113745.

References

[1] A.H. Bass, E.H. Gilland, R. Baker, Evolutionary origins for social vocalization in a vertebrate hindbrain–spinal compartment, Science 321 (2008) 417–421, https://doi.org/10.1126/science.1157632.
[2] J.L. Goodson, The vertebrate social behavior network: evolutionary themes and variations, Horm. Behav. 48 (2005) 11–22, https://doi.org/10.1016/j.yhbeh.2005.02.003.
[3] J.L. Goodson, D. Kabelik, Dynamic limbic networks and social diversity in vertebrates: from neural context to neuromodulatory patterning, Front. Neuroendocrinol. 30 (2009) 429–441, https://doi.org/10.1016/j.yfrne.2009.05.007.
[4] J.L. Goodson, M.A. Kingsbury, What's in a name? Considerations of homologies and nomenclature for vertebrate social behavior networks, Horm. Behav. 64 (2013) 103–112, https://doi.org/10.1016/j.yhbeh.2013.05.006.
[5] S.W. Newman, The medial extended amygdala in male reproductive behavior a node in the mammalian social behavior network, Ann. N. Y. Acad. Sci. 877 (1999) 242–257, https://doi.org/10.1111/j.1749-6632.1999.tb09271.x.
[6] L.A. O'Connell, H.A. Hofmann, The vertebrate mesolimbic reward system and social behavior network: a comparative synthesis, J. Comp. Neurol. 519 (2011) 3599–3639, https://doi.org/10.1002/cne.22735.
[7] L.A. O'Connell, H.A. Hofmann, Evolution of a vertebrate social decision-making network, Science 336 (2012) 1154–1157, https://doi.org/10.1126/science.1218889.
[8] J.M.S. Ellis, L.V. Riters, Patterns of phosphorylated tyrosine hydroxylase vary with song production in female starlings, Brain Res 1498 (2013) 41–49, https://doi.org/10.1016/j.brainres.2012.12.020.
[9] D.P. Merullo, C.S. Angyal, S.A. Stevenson, L.V. Riters, Song in an affiliative context relates to the neural expression of dopamine- and neurotensin-related genes in male european starlings, Brain. Behav. Evol. 88 (2016) 81–92, https://doi.org/10.1159/000448191.
[10] K.S. Lynch, B. Diekamp, G.F. Ball, Catecholaminergic cell groups and vocal communication in male songbirds, Physiol. Behav. 93 (2008) 870–876, https://doi.org/10.1016/j.physbeh.2007.12.004.
[11] J.L. Goodson, D. Kabelik, A.M. Kelly, J. Rinaldi, J.D. Klatt, Midbrain dopamine neurons reflect affiliation phenotypes in finches and are tightly coupled to courtship, Proc. Natl. Acad. Sci. 106 (2009) 8737–8742. ⟨https://doi.org/10.1073/pnas.0811821106⟩.
[12] L.V. Riters, M. Eens, R. Pinxten, G.F. Ball, Seasonal changes in the densities of α2-noradrenergic receptors are inversely related to changes in testosterone and the volumes of song control nuclei in male European starlings, J. Comp. Neurol. 444 (2002) 63–74, https://doi.org/10.1002/cne.10131.
[13] S.A. Heimovics, C.A. Cornil, J.M.S. Ellis, G.F. Ball, L.V. Riters, Seasonal and individual variation in singing behavior correlates with alpha 2-noradrenergic receptor density in brain regions implicated in song, sexual, and social behavior, Neuroscience 182 (2011) 133–143, https://doi.org/10.1016/j.neuroscience.2011.03.012.
[14] Z.P. Sheldon, C.B. Castelino, C.M. Glaze, S.P. Bibu, E. Yau, M.F. Schmidt, Regulation of vocal precision by noradrenergic modulation of a motor nucleus, J. Neurophysiol. 124 (2020) 458–470, https://doi.org/10.1152/jn.00154.2020.
[15] C.A. Kelm-Nelson, M.A. Trevino, M.R. Ciucci, Quantitative analysis of catecholamines in the Pink1 −/− rat model of early-onset Parkinson disease, Neuroscience 379 (2018) 126–141, https://doi.org/10.1016/j.neuroscience.2018.02.027.
[16] J.D. Hoffmeister, C.A. Kelm-Nelson, M.R. Ciucci, Quantification of brainstem norepinephrine relative to vocal impairment and anxiety in the Pink1-/- rat model of Parkinson disease, Behav. Brain Res. 414 (2021), 113514, https://doi.org/10.1016/j.bbr.2021.113514.
[17] A.H. Bass, J.R. McKibben, Neural mechanisms and behaviors for acoustic communication in teleost fish, Prog. Neurobiol. 69 (2003) 1–26, https://doi.org/10.1016/S0301-0082(03)00004-2.
[18] P.M. Forlano, J.A. Sisneros, K.N. Rohmann, A.H. Bass, Neuroendocrine control of seasonal plasticity in the auditory and vocal systems of fish, Front. Neuroendocrinol. 37 (2015) 129–145, https://doi.org/10.1016/j.yfrne.2014.08.002.
[19] A.H. Bass, P.M. Forlano, Neuroendocrine mechanisms of alternative reproductive tactics: the chemical language of reproductive and social plasticity, in: R. F. Oliveira, et al. (Eds.), Altern. Reprod. Tactics, Cambridge University Press, 2008, pp. 109–131.
[20] R.K. Brantley, A.H. Bass, Alternative Male Spawning Tactics and Acoustic Signals in the Plainfin Midshipman Fish Porichthys notatus Girard (Teleostei, Batrachoididae), Ethology 96 (1994) 213–232, https://doi.org/10.1111/j.1439-0310.1994.tb01011.x.
[21] N.Y. Feng, A.H. Bass, 2.04 - Neural, Hormonal, and Genetic Mechanisms of Alternative Reproductive Tactics: Vocal Fish as Model Systems, in: D.W. Pfaff, M. Joëls (Eds.), Horm. Brain Behav, Third ed..,, Academic Press, Oxford, 2017, pp. 47–68, https://doi.org/10.1016/B978-0-12-803592-4.00018-3.
[22] J.L. Goodson, A.H. Bass, Vocal–acoustic circuitry and descending vocal pathways in teleost fish: convergence with terrestrial vertebrates reveals conserved traits, J. Comp. Neurol. 448 (2002) 298–322, https://doi.org/10.1002/cne.10258.
[23] A.H. Bass, B.P. Chagnaud, N.Y. Feng, Comparative Neurobiology of Sound Production in Fishes, in: F. Ladich (Ed.), Sound Commun. Fishes, Springer, Vienna, 2015, pp. 35–75, https://doi.org/10.1007/978-3-7091-1846-7_2.
[24] A.H. Bass, R. Baker, Sexual dimorphisms in the vocal control system of a teleost fish: morphology of physiologically identified neurons, J. Neurobiol. 21 (1990) 1155–1168, https://doi.org/10.1002/neu.480210802.
[25] A.H. Bass, M.A. Marchaterre, R. Baker, Vocal-acoustic pathways in a teleost fish, J. Neurosci. 14 (1994) 4025–4039.
[26] B.P. Chagnaud, R. Baker, A.H. Bass, Vocalization frequency and duration are coded in separate hindbrain nuclei, Nat. Commun. 2 (2011) 346, https://doi.org/10.1038/ncomms1349.
[27] C.B. Castelino, G.F. Ball, A role for norepinephrine in the regulation of context-dependent ZENK expression in male zebra finches (Taeniopygia guttata), Eur. J. Neurosci. 21 (2005) 1962–1972, https://doi.org/10.1111/j.1460-9568.2005.04028.x.
[28] E. Hara, L. Kubikova, N.A. Hessler, E.D. Jarvis, Role of the midbrain dopaminergic system in modulation of vocal brain activation by social context, Eur. J. Neurosci. 25 (2007) 3406–3416, https://doi.org/10.1111/j.1460-9568.2007.05600.x.
[29] P.M. Forlano, Z.N. Ghahramani, C.M. Monestime, P. Kurochkin, A. Chernenko, D. Milkis, Catecholaminergic Innervation of Central and Peripheral Auditory Circuitry Varies with Reproductive State in Female Midshipman Fish, Porichthys notatus, PLOS ONE 10 (2015), e0121914, https://doi.org/10.1371/journal.pone.0121914.
[30] P.M. Forlano, S.D. Kim, Z.M. Krzyminska, J.A. Sisneros, Catecholaminergic connectivity to the inner ear, central auditory, and vocal motor circuitry in the plainfin midshipman fish Porichthys notatus, J. Comp. Neurol. 522 (2014) 2887–2927, https://doi.org/10.1002/cne.23596.
[31] P.M. Forlano, M. Marchaterre, D.L. Deitcher, A.H. Bass, Distribution of androgen receptor mRNA expression in vocal, auditory, and neuroendocrine circuits in a teleost fish, J. Comp. Neurol. 518 (2010) 493–512, https://doi.org/10.1002/cne.22233.
[32] P.M. Forlano, D.L. Deitcher, A.H. Bass, Distribution of estrogen receptor alpha mRNA in the brain and inner ear of a vocal fish with comparisons to sites of aromatase expression, J. Comp. Neurol. 483 (2005) 91–113, https://doi.org/10.1002/cne.20397.
[33] L. Remage-Healey, A.H. Bass, Rapid, hierarchical modulation of vocal patterning by steroid hormones, J. Neurosci. 24 (2004) 5892–5900, https://doi.org/10.1523/JNEUROSCI.1220-04.2004.
[34] L. Remage-Healey, A.H. Bass, Plasticity in brain sexuality is revealed by the rapid actions of steroid hormones, J. Neurosci. 27 (2007) 1114–1122, https://doi.org/10.1523/JNEUROSCI.4282-06.2007.
[35] R.M. Genova, M.A. Marchaterre, R. Knapp, D. Fergus, A.H. Bass, Glucocorticoid and androgen signaling pathways diverge between advertisement calling and non-calling fish, Horm. Behav. 62 (2012) 426–432, https://doi.org/10.1016/j.yhbeh.2012.07.010.
[36] C. Barth, A. Villringer, J. Sacher, Sex hormones affect neurotransmitters and shape the adult female brain during hormonal transition periods, Front. Neurosci. 9 (2015), https://doi.org/10.3389/fnins.2015.00037.
[37] L.L. Matragrano, M.M. LeBlanc, A. Chitrapu, Z.E. Blanton, D.L. Maney, Testosterone alters genomic responses to song and monoaminergic innervation of

auditory areas in a seasonally breeding songbird, Dev. Neurobiol. 73 (2013) 455–468, https://doi.org/10.1002/dneu.22072.
[38] F.-A. Weltzien, C. Pasqualini, M.-E. Sébert, B. Vidal, N. Le Belle, O. Kah, P. Vernier, S. Dufour, Androgen-dependent stimulation of brain dopaminergic systems in the Female European Eel (Anguilla anguilla), Endocrinology 147 (2006) 2964–2973, https://doi.org/10.1210/en.2005-1477.
[39] W. Wilczynski, E.-J. Yang, D. Simmons, Sex differences and hormone influences on tyrosine hydroxylase immunoreactive cells in the leopard frog, J. Neurobiol. 56 (2003) 54–65, https://doi.org/10.1002/neu.10228.
[40] G.F. Ball, C.B. Castelino, D.L. Maney, D. Appeltants, J. Balthazart, The activation of birdsong by testosterone, Ann. N. Y. Acad. Sci. 1007 (2003) 211–231, https://doi.org/10.1196/annals.1286.021.
[41] P.M. Forlano, R.R. Licorish, Z.N. Ghahramani, M. Timothy, M. Ferrari, W. C. Palmer, J.A. Sisneros, Attention and motivated response to simulated male advertisement call activates forebrain dopaminergic and social decision-making network nuclei in female midshipman fish, icx053, Integr. Comp. Biol. (2017), https://doi.org/10.1093/icb/icx053.
[42] Z.N. Ghahramani, M. Timothy, J. Varughese, J.A. Sisneros, P.M. Forlano, Dopaminergic neurons are preferentially responsive to advertisement calls and co-active with social behavior network nuclei in sneaker male midshipman fish, Brain Res. 2018 (1701) 177–188, https://doi.org/10.1016/j.brainres.2018.09.014.
[43] R.A. Mohr, Y. Chang, A.A. Bhandiwad, P.M. Forlano, J.A. Sisneros, Brain activation patterns in response to conspecific and heterospecific social acoustic signals in female plainfin midshipman fish, porichthys notatus, Brain. Behav. Evol. 91 (2018) 31–44, https://doi.org/10.1159/000487122.
[44] C.L. Petersen, M. Timothy, D.S. Kim, A.A. Bhandiwad, R.A. Mohr, J.A. Sisneros, P. M. Forlano, Exposure to advertisement calls of reproductive competitors activates vocal-acoustic and catecholaminergic neurons in the plainfin midshipman fish, porichthys notatus, PLOS ONE 8 (2013), e70474, https://doi.org/10.1371/journal.pone.0070474.
[45] E.L. McIver, M.A. Marchaterre, A.N. Rice, A.H. Bass, Novel underwater soundscape: acoustic repertoire of plainfin midshipman fish, J. Exp. Biol. 217 (2014) 2377–2389, https://doi.org/10.1242/jeb.102772.
[46] J.A. Sisneros, P.W. Alderks, K. Leon, B. Sniffen, Morphometric changes associated with the reproductive cycle and behaviour of the intertidal-nesting, male plainfin midshipman Porichthys notatus, J. Fish. Biol. 74 (2009) 18–36, https://doi.org/10.1111/j.1095-8649.2008.02104.x.
[47] A.H. Bass, D.A. Bodnar, M.A. Marchaterre, Complementary explanations for existing phenotypes in an acoustic communication system, in: M.D. Hauser, M. Konishi (Eds.), Des. Anim. Commun., 1999, pp. 493–514.
[48] R.M. Ibara, L.T. Penny, A.W. Ebeling, G. van Dykhuizen, G. Cailliet, The mating call of the plainfin midshipman fish, Porichthys notatus, in: Predat. Prey Fishes, Springer, Dordrecht, 1983, pp. 205–212, https://doi.org/10.1007/978-94-009-7296-4_22.
[49] A.H. Bass, M.A. Marchaterre, Sound-generating (sonic) motor system in a teleost fish (Porichthys notatus): sexual polymorphisms and general synaptology of sonic motor nucleus, J. Comp. Neurol. 286 (1989) 154–169, https://doi.org/10.1002/cne.902860203.
[50] Z.N. Ghahramani, M. Timothy, G. Kaur, M. Gorbonosov, A. Chernenko, P. M. Forlano, Catecholaminergic fiber innervation of the vocal motor system is intrasexually dimorphic in a teleost with alternative reproductive tactics, Brain. Behav. Evol. 86 (2015) 131–144, https://doi.org/10.1159/000438720.
[51] A.M. Kelly, J.L. Goodson, Functional interactions of dopamine cell groups reflect personality, sex, and social context in highly social finches, Behav. Brain Res. 280 (2015) 101–112, https://doi.org/10.1016/j.bbr.2014.12.004.
[52] M. Timothy, P.M. Forlano, A versatile macro-based neurohistological image analysis suite for ImageJ focused on automated and standardized user interaction and reproducible data output, J. Neurosci. Methods 324 (2019), 108286, https://doi.org/10.1016/j.jneumeth.2019.04.009.
[53] Y. Benjamini, Y. Hochberg, Controlling the false discovery rate: a practical and powerful approach to multiple, Test., J. R. Stat. Soc. Ser. B Method. 57 (1995) 289–300.
[54] J.M. Butler, K.P. Maruska, The mechanosensory lateral line system mediates activation of socially-relevant brain regions during territorial interactions, Front. Behav. Neurosci. 10 (2016), https://doi.org/10.3389/fnbeh.2016.00093.
[55] S. Borgatti, M. Everett, L. Freeman, Ucinet for Windows: Software for Social Network Analysis, Analytic Technologies, 2002.
[56] M.M. Makagon, B. McCowan, J.A. Mench, How can social network analysis contribute to social behavior research in applied ethology? Appl. Anim. Behav. Sci. 138 (2012) 152–161, https://doi.org/10.1016/j.applanim.2012.02.003.
[57] N. So, B. Franks, S. Lim, J.P. Curley, A social network approach reveals associations between mouse social dominance and brain gene expression, PLOS ONE 10 (2015), e0134509, https://doi.org/10.1371/journal.pone.0134509.
[58] O. Almeida, A.S. Félix, G.A. Oliveira, J.S. Lopes, R.F. Oliveira, Fighting assessment triggers rapid changes in activity of the brain social decision-making network of Cichlid fish, Front. Behav. Neurosci. 13 (2019), https://doi.org/10.3389/fnbeh.2019.00229.
[59] A. Roleira, G.A. Oliveira, J.S. Lopes, R.F. Oliveira, Audience effects in territorial defense of male cichlid fish are associated with differential patterns of activation of the brain social decision-making network, Front. Behav. Neurosci. 11 (2017), https://doi.org/10.3389/fnbeh.2017.00105.
[60] M.C. Teles, O. Almeida, J.S. Lopes, R.F. Oliveira, Social interactions elicit rapid shifts in functional connectivity in the social decision-making network of zebrafish, Proc R Soc B. 282 (2015) 20151099. ⟨https://doi.org/10.1098/rspb.2015.1099⟩.
[61] M. Bastian, S. Heymann, M. Jacomy, Gephi: An Open Source Software for Exploring and Manipulating Networks, in: Third Int. AAAI Conf. Weblogs Soc. Media, 2009. ⟨https://www.aaai.org/ocs/index.php/ICWSM/09/paper/view/154⟩ (accessed March 17, 2018).
[62] T. Okuyama, Y. Suehiro, H. Imada, A. Shimada, K. Naruse, H. Takeda, T. Kubo, H. Takeuchi, Induction of c-fos transcription in the medaka brain (Oryzias latipes) in response to mating stimuli, Biochem. Biophys. Res. Commun. 404 (2011) 453–457, https://doi.org/10.1016/j.bbrc.2010.11.143.
[63] W.J.A.J. Smeets, A. González, Catecholamine systems in the brain of vertebrates: new perspectives through a comparative approach, Brain Res. Rev. 33 (2000) 308–379, https://doi.org/10.1016/S0165-0173(00)00034-5.
[64] T.L. Tay, O. Ronneberger, S. Ryu, R. Nitschke, W. Driever, Comprehensive catecholaminergic projectome analysis reveals single-neuron integration of zebrafish ascending and descending dopaminergic systems, Nat. Commun. 2 (2011) 171, https://doi.org/10.1038/ncomms1171.
[65] N. Farassat, K.M. Costa, S. Stojanovic, S. Albert, L. Kovacheva, J. Shin, R. Egger, M. Somayaji, S. Duvarci, G. Schneider, J. Roeper, In vivo functional diversity of midbrain dopamine neurons within identified axonal projections, ELife 8 (2019), e48408, https://doi.org/10.7554/eLife.48408.
[66] C.L. Petersen, S.E.D. Davis, B. Patel, L.M. Hurley, Social experience interacts with serotonin to affect functional connectivity in the social behavior network following playback of social vocalizations in mice, ENeuro 8 (2021), https://doi.org/10.1523/ENEURO.0247-20.2021.
[67] T. Mueller, S. Guo, The distribution of GAD67-mRNA in the adult zebrafish (teleost) forebrain reveals a prosomeric pattern and suggests previously unidentified homologies to tetrapods, J. Comp. Neurol. 516 (2009) 553–568, https://doi.org/10.1002/cne.22122.
[68] M. Timothy, P.M. Forlano, Immunohistochemical localization of GABA and serotonin provides an emerging picture of neuromodulator interactivity in a vocal teleost, 584.10, Neuroscience Meeting Planner, San Diego, CA, 2013.
[69] J.M. Kittelberger, B.R. Land, A.H. Bass, Midbrain periaqueductal gray and vocal patterning in a Teleost Fish, J. Neurophysiol. 96 (2006) 71–85, https://doi.org/10.1152/jn.00067.2006.
[70] J.M. Kittelberger, A.H. Bass, Vocal-motor and auditory connectivity of the midbrain periaqueductal gray in a teleost fish, J. Comp. Neurol. 521 (2013) 791–812, https://doi.org/10.1002/cne.23202.
[71] E. Rink, M.F. Wullimann, The teleostean (zebrafish) dopaminergic system ascending to the subpallium (striatum) is located in the basal diencephalon (posterior tuberculum), Brain Res 889 (2001) 316–330, https://doi.org/10.1016/S0006-8993(00)03174-7.
[72] L.E. Matheson, J.T. Sakata, Catecholaminergic contributions to vocal communication signals, Eur. J. Neurosci. 41 (2015) 1180–1194, https://doi.org/10.1111/ejn.12885.
[73] S.R. Barclay, C.F. Harding, S.A. Waterman, Central DSP-4 treatment decreases norepinephrine levels and courtship behavior in male zebra finches, Pharmacol. Biochem. Behav. 53 (1996) 213–220, https://doi.org/10.1016/0091-3057(95)00183-2.
[74] J.D. Hoffmeister, C.A. Kelm-Nelson, M.R. Ciucci, Manipulation of vocal communication and anxiety through pharmacologic modulation of norepinephrine in the Pink1-/- rat model of Parkinson disease, Behav. Brain Res. 418 (2022), 113642, https://doi.org/10.1016/j.bbr.2021.113642.
[75] J.L. Goodson, A.H. Bass, Forebrain peptides modulate sexually polymorphic vocal circuitry, Nature 403 (2000) 769–772, https://doi.org/10.1038/35001581.
[76] J.L. Goodson, A.H. Bass, Rhythmic midbrain-evoked vocalization is inhibited by vasoactive intestinal polypeptide in the teleost Porichthys notatus, Brain Res 865 (2000) 107–111, https://doi.org/10.1016/s0006-8993(00)02232-0.
[77] J.L. Goodson, A.H. Bass, Vasotocin innervation and modulation of vocal-acoustic circuitry in the teleost Porichthys notatus, J. Comp. Neurol. 422 (2000) 363–379, https://doi.org/10.1002/1096-9861(20000703)422:3<363::AID-CNE4>3.0.CO;2-8.
[78] N.Y. Feng, A.H. Bass, Melatonin action in a midbrain vocal-acoustic network, J. Exp. Biol. 217 (2014) 1046–1057, https://doi.org/10.1242/jeb.096669.
[79] E.R. Schuppe, M.D. Zhang, J.T. Perelmuter, M.A. Marchaterre, A.H. Bass, Oxytocin-like receptor expression in evolutionarily conserved nodes of a vocal network associated with male courtship in a teleost fish, J. Comp. Neurol. N./a (2021), https://doi.org/10.1002/cne.25257.
[80] J.L. Goodson, A.K. Evans, A.H. Bass, Putative isotocin distributions in sonic fish: Relation to vasotocin and vocal–acoustic circuitry, J. Comp. Neurol. 462 (2003) 1–14, https://doi.org/10.1002/cne.10679.
[81] J.A. Tripp, N.Y. Feng, A.H. Bass, To hum or not to hum: neural transcriptome signature of male courtship vocalization in a teleost fish, Genes Brain Behav. 20 (2021), e12740, https://doi.org/10.1111/gbb.12740.
[82] S. Nakagawa, A farewell to bonferroni: the problems of low statistical power and publication bias, Behav. Ecol. 15 (2004) 1044–1045, https://doi.org/10.1093/beheco/arh107.
[83] D.J. Fergus, A.H. Bass, Localization and divergent profiles of estrogen receptors and aromatase in the vocal and auditory networks of a fish with alternative mating tactics, J. Comp. Neurol. 521 (2013) 2850–2869, https://doi.org/10.1002/cne.23320.
[84] P.M. Forlano, D.L. Deitcher, D.A. Myers, A.H. Bass, Anatomical distribution and cellular basis for high levels of aromatase activity in the brain of teleost fish: aromatase enzyme and mrna expression identify glia as source, J. Neurosci. 21 (2001) 8943–8955.
[85] N.Y. Feng, M.A. Marchaterre, A.H. Bass, Melatonin receptor expression in vocal, auditory, and neuroendocrine centers of a highly vocal fish, the plainfin midshipman (Porichthys notatus), J. Comp. Neurol. 527 (2019) 1362–1377, https://doi.org/10.1002/cne.24629.

[86] N.Y. Feng, A.H. Bass, "Singing" Fish Rely on Circadian Rhythm and Melatonin for the Timing of Nocturnal Courtship Vocalization, Curr. Biol. 26 (2016) 2681–2689, https://doi.org/10.1016/j.cub.2016.07.079.
[87] A.H. Bass, D.A. Bodnar, M.A. Marchaterre, Midbrain acoustic circuitry in a vocalizing fish, J. Comp. Neurol. 419 (2000) 505–531, https://doi.org/10.1002/(SICI)1096-9861(20000417)419:4<505::AID-CNE7>3.0.CO;2-3.
[88] G.K.E. Goebrecht, R.A. Kowtoniuk, B.G. Kelly, J.M. Kittelberger, Sexually-dimorphic expression of tyrosine hydroxylase immunoreactivity in the brain of a vocal teleost fish (Porichthys notatus), J. Chem. Neuroanat. 56 (2014) 13–34, https://doi.org/10.1016/j.jchemneu.2014.01.001.
[89] C. Maximino, M.G. Lima, K.R.M. Oliveira, E. de, J.O. Batista, A.M. Herculano, "Limbic associative" and "autonomic" amygdala in teleosts: A review of the evidence, J. Chem. Neuroanat. 48 (2013) 1–13, https://doi.org/10.1016/j.jchemneu.2012.10.001.
[90] T. Mueller, M.F. Wullimann, An evolutionary interpretation of teleostean forebrain anatomy, Brain. Behav. Evol. 74 (2009) 30–42, https://doi.org/10.1159/000229011.
[91] M.F. Wullimann, T. Mueller, Teleostean and mammalian forebrains contrasted: evidence from genes to behavior, J. Comp. Neurol. 475 (2004) 143–162, https://doi.org/10.1002/cne.20183.
[92] L.L. Bruce, M.R. Braford Jr., Evolution of the Limbic System, in: L.R. Squire (Ed.), Encycl. Neurosci., Academic Press, Oxford, 2009, pp. 43–55, https://doi.org/10.1016/B978-008045046-9.00965-7.
[93] R.G. Northcutt, The forebrain of gnathostomes: in search of a morphotype, Brain. Behav. Evol. 46 (304–318) (1995) 304–318, https://doi.org/10.1159/000113281.
[94] K. Yamamoto, P. Vernier, The evolution of dopamine systems in chordates, Front. Neuroanat. 5 (2011) 21, https://doi.org/10.3389/fnana.2011.00021.
[95] T. Hökfelt, R. Mårtensson, Distributional maps of tyrosine-hydroxylase-immunoreactive neurons in the rat brain, in: A. Björklund, T. Hökfelt (Eds.), Handb. Chem. Neuroanat. Part Vol 2 Class. Transm. CNS, Elsevier, 1984, pp. 277–379.
[96] J. Kaslin, P. Panula, Comparative anatomy of the histaminergic and other aminergic systems in zebrafish (Danio rerio), J. Comp. Neurol. 440 (2001) 342–377, https://doi.org/10.1002/cne.1390.
[97] F.L. Moore, C.A. Lowry, Comparative neuroanatomy of vasotocin and vasopressin in amphibians and other vertebrates, Comp. Biochem. Physiol. C. Pharmacol. Toxicol. Endocrinol. 119 (1998) 251–260, https://doi.org/10.1016/S0742-8413(98)00014-0.